CIRRELT

CIRRELT-2026-16

A Single-Truck-Single-Drone Collaborative Routing under a Decentralized Battery-Swapping Strategy

Qing Liu
Wenjing Guo
Frederik Schulte
Teodor Gabriel Crainic

Août 2026

Bureau de Montréal
Université de Montréal
C.P. 6128, succ. Centre-Ville
Montréal (Québec) H3C 3J7
Tél : 1-514-343-7575
Télécopie : 1-514-343-7121

Bureau de Québec
Université Laval,
2325, rue de la Terrasse
Pavillon Palasis-Prince, local 2415
Québec (Québec) G1V 0A6
Tél : 1-418-656-2073
Télécopie : 1-418-656-2624

A Single-Truck-Single-Drone Collaborative Routing under a Decentralized Battery-Swapping Strategy

Qing Liu[1], Wenjing Guo[1], Frederik Schulte[2], Teodor Gabriel Crainic[3*]

[1] Wuhan University of Technology, Wuhan, China

[2] Delft University of Technology, Delft, The Netherlands

[3] Université du Québec à Montréal and Interuniversity Research Centre on Enterprise Networks, Logistics and Transportation (CIRRELT), Montréal, Canada

Abstract. This paper investigates a single-truck-single-drone collaborative routing problem for the pickup of fresh agricultural products in mountainous areas. Existing models largely rely on trucks as the only mobile energy hubs for drones, resulting in a tightly coupled routing framework for trucks and drones. This design severely limits the operational range of drones and lacks the spatial flexibility needed to accommodate the rapid quality decay of perishable goods during collection. To overcome these spatial constraints, this paper develops a single-truck-single-drone collaborative routing model under a decentralized battery-swapping strategy. Deploying cost-effective energy relay nodes directly at farm pickup points, we establish a dual replenishment network integrating dynamic battery swaps on mobile trucks with fixed swaps at farm locations. This fundamentally decouples the drone's spatial reliance on the truck. Experimental results show that, facilitated by the continuous multi-visit capabilities and the decentralized battery-swapping mechanism, the routing network topology can dynamically adapt under extreme asymmetric payloads.

Keywords: Truck-drone collaborative routing; Decentralized battery-swapping strategy; Quality decay dynamics; Load-aware power consumption.

Acknowledgements. This research is supported by the National Natural Science Foundation of China under Grants 72301203 and U2572211. While working on the project, T.G. Crainic was Adjunct Professor in the Department of Computer Science and Operations Research at the Université de Montréal.

---

* Corresponding author: : teodorgabriel.crainic@cirrelt.net

Dépôt légal – Bibliothèque et Archives nationales du Québec

Bibliothèque et Archives Canada, 2026

1 Introduction

The efficient "first-mile" collection of fresh agricultural products in mountainous regions is heavily constrained by sparse road networks. Traditional trucks cannot reach remote farms, leading to prolonged transit and rapid quality decay. While Unmanned Aerial Vehicle (UAV) offer direct access and rapid response, their application is severely bottlenecked by short flight ranges and limited payloads. Therefore, integrating the trunk-line endurance of trucks with the terminal maneuverability of UAV offers a highly promising paradigm for perishable goods logistics.

Research on vehicle-drone collaborative delivery has established a substantial theoretical foundation. Classical models, such as the Flying Sidekick Traveling Salesman Problem (FSTSP) [1] for single-truck-single-drone operations and the Vehicle Routing Problem with Drones (VRP-D) [2] for multi-truck-multi-drone operations, primarily aim to minimize time [3-4] or distance costs [5-6]. Some studies have incorporated the perishability of fresh produce, formulating it either as time window constraints [7-8] or spoilage cost functions [9]. Recent routing models have incorporated temperature-dependent degradation based on Arrhenius kinetics [10], to address the rapid quality decay of perishable goods. Regarding energy constraints, most studies simplify UAV power consumption as a linear function of flight distance [11-12]. A more refined, load-aware power consumption model has been proposed to account for the impact of payload variations on energy depletion [13-14]. However, existing models generally rely on mid-route rendezvous with trucks for battery swapping or recharging to extend UAV operation [15-16]. This prevailing "swap-on-return" paradigm intrinsically tethers the drone's spatial range to the truck's physical location, lacking an independent energy replenishment mechanism to sustain continuous, wide-area operations across complex mountainous terrains.

To address this methodological gap, this paper formulates an optimization model for a single-truck-single-drone collaborative routing under a decentralized battery-swapping strategy. Building upon existing load-aware energy models and Arrhenius quality decay dynamics, our core contribution is the design of a dual replenishment network. This architecture integrates dynamic battery swapping on mobile trucks with fixed, independent battery swapping at remote mountainous farms. Crucially, the on-site battery replacement at remote farms is strictly executed when the UAV is launched for its next leg, rather than relying on its return to the truck. This strategy fundamentally overcomes the spatial restrictions of the truck's operational radius, completely unlocking the UAV's potential for extended multi-visit routing and expanding the overall operational range of the collaborative network.

2 Problem description

The logistics network investigated in this paper is modeled as a directed graph $G = (N, A)$. The logistics network comprises the cold-storage depot (starting and ending nodes), the set of roadside farms be serviced by the truck, and the set of remote mountainous farms be serviced by the UAV.

(1) Truck: Serving as a mobile cold-chain compartment and energy hub, its physical trajectories are strictly confined to the primary road network.

(2) UAV: Utilizing the truck as a mobile launch and recovery platform, the UAV is tasked with traversing complex terrains to execute first-mile collection at nodes within N_{drone}. While being transported by the truck along the primary road network, the UAV remains in a $"carried"$ state.

To fundamentally overcome the "radius lock-in" bottleneck inherent in the truck's battery-swapping systems and to fully unlock the spatial flexibility of the UAV in expansive mountainous terrains, this study proposes a decentralized battery swapping strategy:

(1) Mechanism A: The truck serves as a mobile charging hub, featuring an onboard energy pool. The system dynamically replenishes energy at a rated power during the truck's transit. Upon launching from roadside farms, the UAV swaps its depleted battery directly via the truck's energy pool.

(2) Mechanism B: Pre-deployed battery-swapping resources are situated at all remote mountainous farms. This mechanism allows the UAV to swaps batteries without returning to the truck, providing the necessary physical framework for cross-regional "multi-visit routing."

To guarantee mathematical rigor and physical feasibility, the proposed model is grounded in the following core assumptions:

(1) The collection demand at each farm node must be fulfilled entirely by a single visit from one vehicle.

(2) All farms are assumed to possess the requisite conditions for UAV landings. While awaiting truck recovery at a rendezvous node, the UAV remains in a grounded standby mode. During this period, the UAV's energy consumption is assumed to be negligible, and only the quality decay of the onboard fresh produce is accumulated.

(3) Upon the UAV's retrieval by the truck, the offloading and transfer of fresh produce into the cold-chain compartment are assumed to be executed instantaneously. Consequently, the transition of the cargo from the UAV's ambient temperature exposure phase to the truck's low-temperature preservation phase incurs zero-time penalty, and any thermal exchange losses during this transfer are disregarded.

(4) The spatial flight trajectory of the UAV is approximated by the 2D Euclidean distance, and it operates at a constant rated speed under steady-state cruising conditions. Transient energy consumption surges induced by takeoff climbing, landing hovering, and acceleration/deceleration phases are neglected.

(5) The truck's onboard dynamic charging system is active during the transit phase, charging the energy pool at a constant rated power.

3 Mathematical Formulation

This section formulates the single-truck-single-drone collaborative routing problem for first-mile fresh product collection, incorporating the dual replenishment mechanism, as a Mixed Integer Linear Programming (MILP) model.

3.1 Notation

The sets, parameters, and variables used in the model are summarized in Table 1.

Table 1. Notation.

Sets:	
N	Set of all network nodes
N_{truck}	Set of nodes accessible by the truck
N_{truck}^{R}	Set of roadside farms
N_{drone}	Set of remote mountainous farms accessible by the UAV
Economic and Value Parameters:	
$C_{time}^{truck}, C_{wait}^{truck}$	Unit time cost for truck travel and waiting
C_{time}^{drone}	Unit flight cost of the UAV
C_{swap}	Unit cost of a single battery-swapping operation and consumables
P_i	Initial unit value of fresh produce at node i

Physical and Temporal Parameters:	
q_i	Collection demand of fresh produce at node i
s_i	Service time required for collection at node i
Q_{truck}, Q_{drone}	Maximum payload capacities of the truck and the UAV
$t_{ij}^{truck}, t_{ij}^{drone}$	Travel times of the truck and the UAV on edge (i,j)
T_{swap}	Duration of a single manual battery-swapping operation
M	A sufficiently large number used for linearizing logical constraints
k_{high}, k_{low}	Quality decay rates of fresh produce under ambient temperature exposure and low-temperature preservation environments
Energy and Aerodynamic Parameters:	
m	Tare weight of the UAV
B_{max}	Maximum energy capacity of a single UAV battery
v_{drone}	Cruising speed of the UAV
η, γ	Propeller transmission efficiency and lift-to-drag ratio
f	Power consumption rate of onboard electronics
g	Gravitational acceleration
E_{pool}^{max}	Maximum physical capacity of the truck's onboard energy pool
P_{charge}	Rated fast-charging power of the truck's onboard charging system
Binary Decision Variables:	
x_{ij}, y_{ij}	Binary variable indicating whether the truck and the UAV traverses arc (i,j)
$carry_{ij}$	Binary variable indicating whether the UAV is in the "carried" state by the truck on arc (i,j)
β_i	Binary variable indicating whether a battery-swapping operation is triggered for the UAV at node i
Continuous Decision Variables:	
A_i^{drone}, A_i^{truck}	Arrival times of the UAV and the truck at node i
D_i^{drone}, D_i^{truck}	Departure times of the UAV and the truck from node i
$Wait_i^{drone}, Wait_i^{truck}$	Waiting time incurred by the UAV and the truck at the rendezvous node for spatio-temporal synchronization
$U_{ij}^{drone}, V_{ij}^{truck}$	Real-time payloads of the UAV and the truck on arc (i,j)
e_{ij}	Energy consumption of the UAV on arc (i,j)
E_i^{arr}, E_i^{dep}	Battery energy levels of the UAV upon arrival at and departure from i

Q_i	Total available energy of the truck upon arrival at node i
T_{high}^i, T_{low}^i	Exposure durations of fresh produce at node i in ambient and low-temperature environments

3.2 Objective Function

The objective of the proposed model is to minimize the total system cost Z, which comprises two primary components: the operational cost Z_{ops} and the fresh produce quality decay cost Z_{loss}, expressed as:

$$\min Z = Z_{ops} + Z_{loss} \tag{1}$$

The operational cost encompasses the costs associated with the truck travel time, the truck's idle waiting time incurred to achieve spatio-temporal synchronization with the UAV, the UAV's flight time, and battery-swapping operations:

$$\begin{aligned} Z_{ops} = &\sum_{(i,j)\in A} C_{time}^{truck} \cdot t_{ij}^{truck} \cdot x_{ij} + \sum_{i\in N_{truck}^R} C_{wait}^{truck} \cdot Wait_i^{truck} \\ &+ \sum_{(i,j)\in A} C_{time}^{drone} \cdot t_{ij}^{drone} \cdot y_{ij} + \sum_{i\in N} C_{swap} \cdot \beta_i \end{aligned} \tag{2}$$

This study partitions the collection process into two distinct heterogeneous environmental phases: (1) Ambient Temperature Exposure Phase, which encompasses the durations of UAV flight, farm-site service operations, and landing standby synchronization at the rendezvous node, corresponding to a relatively high quality decay rate. (2) Low-Temperature Preservation Phase, which represents the transit time from the moment the fresh produce is loaded into the truck's cold-chain compartment until its arrival at the destination depot, corresponding to an exceptionally low quality decay rate. The fresh produce quality decay cost is formulated based on the first-order Arrhenius kinetics equation and subsequently linearly approximated, accurately capturing the cumulative economic value depreciation of the fresh produce across both the ambient temperature exposure phase and the truck's low-temperature preservation phase:

$$Z_{loss} = \sum_{i\in N} P_i \cdot q_i \cdot \left(1 - e^{-\left(k_{high}\cdot T_{high}^i + k_{low}\cdot T_{low}^i\right)}\right) \approx \sum_{i\in N} P_i \cdot q_i \cdot \left(k_{high} \cdot T_{high}^i + k_{low} \cdot T_{low}^i\right) \tag{3}$$

3.3 Constraints

Truck Spatial Routing Constraints:

$$\sum_{j\in N_{truck}\setminus\{0\}} x_{0,j} = 1 \tag{4}$$

$$\sum_{i\in N_{truck}\setminus\{n+1\}} x_{i,n+1} = 1 \tag{5}$$

$$\sum_{j\in N_{truck}} x_{ji} = \sum_{j\in N_{truck}} x_{ij} = 1, \forall i \in N_{truck}^R \tag{6}$$

Constraints (4) – (6) denote the basic routing and flow conservation constraints for the truck, collectively ensuring that the truck departs unidirectionally from the origin, sequentially visits each roadside farm exactly once, and ultimately terminates at the destination cold storage.

Truck Payload Constraints:

$$V_{ij}^{truck} \leq Q_{truck} \cdot x_{ij}, \forall i,j \in N_{truck} \tag{7}$$

$$V_{0,j}^{truck} = 0, \forall j \in N_{truck} \tag{8}$$

$$\sum_{j \in N_{truck} \setminus \{0\}} V_{ij}^{truck} - \sum_{j \in N_{truck} \setminus \{n+1\}} V_{ji}^{truck} = q_i + \sum_{j \in N_{drone}} U_{ji}^{drone}, \forall i \in N_{truck}^{R} \tag{9}$$

Constraints (7) and (8) define the physical capacity upper bounds and the unladen departure conditions for the truck, respectively. Constraint (9) formulates the dynamic payload flow conservation at the roadside farms: the difference in the truck's payload between departing and entering a given node must be strictly equal to the sum of the local fresh produce supply and the remote mountainous cargo unloaded by the UAV at that node.

Truck Temporal Constraints:

$$A_j^{truck} \geq D_i^{truck} + t_{ij}^{truck} - M(1 - x_{ij}), \forall i,j \in N_{truck} \tag{10}$$

$$A_j^{truck} \leq D_i^{truck} + t_{ij}^{truck} + M(1 - x_{ij}), \forall i,j \in N_{truck} \tag{11}$$

$$D_i^{truck} = A_i^{truck} + s_i + T_{swap} \cdot \beta_i + Wait_i^{truck}, \forall i \in N_{truck}^{R} \tag{12}$$

Constraints (10) and (11) employ the Big-M formulation to enforce the temporal continuity of the truck's travel between adjacent nodes. Constraint (12) formulates the dwell time conservation for the truck at roadside farms, ensuring that its departure time is strictly equal to the arrival time plus the total duration required for local collection, battery-swapping operations, and synchronous idle waiting.

Truck Energy Pool Constraints:

$$Q_0 = E_{pool}^{max} \tag{13}$$

$$\beta_i \cdot B_{max} \leq Q_i \leq E_{pool}^{max}, \forall i \in N_{truck}^{R} \tag{14}$$

$$Q_j \leq Q_i - \beta_i \cdot B_{max} + P_{charge} \cdot t_{ij}^{truck} + M(1 - x_{ij}), \forall i,j \in N_{truck} \tag{15}$$

Constraint (13) ensures that the truck departs from the depot with a fully charged energy pool. Constraint (14) defines the capacity boundaries and the anti-overdischarge safeguard for the truck's energy pool. Constraint (15) precisely evaluates the dynamic energy variation of the truck along its travel arcs.

UAV Spatial Routing Constraints:

$$\sum_{j \in N \setminus \{n+1\}} y_{ji} = \sum_{j \in N \setminus \{0\}} y_{ij} = 1, \forall i \in N_{drone} \tag{16}$$

Constraint (16) defines the standard spatial flow conservation constraint for the UAV at remote mountainous farms, ensuring that each remote node is effectively visited exactly once.

UAV Payload Constraints:

$$U_{ij}^{drone} \leq Q_{drone} \cdot y_{ij}, \forall i,j \in N \tag{17}$$

$$U_{ij}^{drone} = 0, \forall i \in N_{truck}, \forall j \in N \tag{18}$$

$$\sum_{j \in N \setminus \{0\}} U_{ij}^{drone} - \sum_{j \in N \setminus \{n+1\}} U_{ji}^{drone} = q_i, \forall i \in N_{drone} \tag{19}$$

Constraints (17) and (18) establish the physical capacity upper bounds and the unladen launch safeguards for the UAV. Constraint (19) formulates the dynamic payload flow conservation equation at remote mountainous farms, ensuring that the variation in the UAV's payload before and after visiting a node strictly matches the local collection demand.

UAV Battery-Swapping Constraints:

$$e_{ij} = \left(\frac{\left(m + U_{ij}^{drone}\right) \cdot g \cdot v_{drone}}{\eta \cdot \gamma} + f \right) \cdot t_{ij}^{drone}, \forall i, j \in N \tag{20}$$

$$E_j^{arr} \leq E_i^{dep} - e_{ij} + M\left(1 - y_{ij}\right), \forall i, j \in N \tag{21}$$

$$\beta_i = \sum_{j \in N_{drone}} y_{ij}, \forall i \in N_{truck}^R \tag{22}$$

$$E_i^{dep} \geq B_{max} - M(1 - \beta_i), \forall i \in N_{drone} \cup N_{truck}^R \tag{23}$$

$$E_i^{dep} \leq B_{max}, \forall i \in N_{drone} \cup N_{truck}^R \tag{24}$$

$$E_i^{dep} \geq E_i^{arr} - M \cdot \beta_i, \forall i \in N_{drone} \cup N_{truck}^R \tag{25}$$

$$E_i^{dep} \leq E_i^{arr} + M \cdot \beta_i, \forall i \in N_{drone} \cup N_{truck}^R \tag{26}$$

$$E_0^{dep} = B_{max} \tag{27}$$

Under the highly asymmetric payload conditions inherent in first-mile fresh produce collection—typically characterized by empty outbound flights and heavily loaded return flights—traditional distance-based linear energy estimations are highly prone to causing critical flight failures. To guarantee absolute operational safety within complex mountainous environments, this paper incorporates an aerodynamics-based, load-aware UAV power consumption model. Constraint (20) characterizes the coupling relationship between the UAV's physical flight energy consumption and its airborne payload weight. Constraint (21) establishes the recursive energy dissipation equation for the UAV across spatial nodes. Constraint (22) enforces a mandatory battery replacement protocol, dictating that the UAV dispatch from a roadside node towards the remote mountains strictly triggers a battery-swapping action. Constraints (23) – (26) calculate the UAV’s energy with or without battery swapping. Specifically, triggering a battery swap resets the departure energy to full capacity; otherwise, strict continuous conservation is maintained between the arrival and departure energy levels. Constraint (27) guarantees a fully charged initial state for the UAV's inaugural launch.

UAV Temporal Constraints:

$$A_j^{drone} \geq D_i^{drone} + t_{ij}^{drone} - M\left(1 - y_{ij}\right), \forall i, j \in N \tag{28}$$

$$A_j^{drone} \leq D_i^{drone} + t_{ij}^{drone} + M\left(1 - y_{ij}\right), \forall i, j \in N \tag{29}$$

$$D_i^{drone} = A_i^{drone} + s_i + T_{swap} \cdot \beta_i, \forall i \in N_{drone} \tag{30}$$

$$D_i^{drone} \geq A_i^{drone} + T_{swap} \cdot \left(\sum_{k \in N_{drone}} y_{ik} \right) - M\left(1 - \sum_{h \in N_{drone}} y_{hi}\right) - M \sum_{j \in N_{truck}} carry_{ji}, \forall i \in N_{truck}^{R} \tag{31}$$

Constraints (28) and (29) formulate the temporal continuity constraints for the UAV's flight operations. Constraint (30) defines the dwell time of the UAV at remote mountainous farms. Constraint (31) acts as a departure timing safeguard for the UAV at roadside nodes.

Spatial Coupling Constraints:

$$carry_{ij} \leq x_{ij}, \forall i, j \in N_{truck} \tag{32}$$

$$\sum_{j \in N_{drone}} y_{0,j} + \sum_{j \in N_{truck}} carry_{0,j} = 1 \tag{33}$$

$$\sum_{i \in N_{drone}} y_{i,n+1} + \sum_{i \in N_{truck}} carry_{i,n+1} = 1 \tag{34}$$

$$\sum_{j \in N_{drone}} y_{ji} + \sum_{j \in N_{truck}} carry_{ji} = \sum_{j \in N_{drone}} y_{ij} + \sum_{j \in N_{truck}} carry_{ij}, \forall i \in N_{truck}^{R} \tag{35}$$

Constraint (32) establishes the physical dependency safeguard for the UAV, permitting it to be piggybacked exclusively along truck routing segments. Constraints (33) and (34) ensure that the UAV enters and exits the cold storage depot either via direct flight or by being transported onboard the truck. Constraint (35) formulates the macroscopic truck-drone collaborative flow conservation at roadside farms, ensuring that the inflow and outflow across all physical flight and piggybacked states are strictly equal.

Temporal Synchronization and Coupling Constraints:

$$D_0^{truck} = D_0^{drone} = 0 \tag{36}$$

$$D_i^{drone} \geq A_i^{truck} + T_{swap} - M\left(1 - \sum_{j \in N_{drone}} y_{ij}\right), \forall i \in N_{truck}^{R} \tag{37}$$

$$D_i^{drone} \leq D_i^{truck} + M\left(1 - \sum_{j \in N_{drone}} y_{ij}\right), \forall i \in N_{truck}^{R} \tag{38}$$

$$Wait_i^{drone} \geq A_i^{truck} - A_i^{drone} - M \cdot \left(1 - \sum_{j \in N_{drone}} y_{ji}\right), \forall i \in N_{truck}^{R} \tag{39}$$

$$Wait_i^{truck} \geq A_i^{drone} - A_i^{truck} - s_i - M \cdot \left(1 - \sum_{j \in N_{drone}} y_{ji}\right), \forall i \in N_{truck}^{R} \tag{40}$$

Constraint (36) establishes the origin of the global time axis. Constraints (37) and (38) strictly confine the UAV's launch operations within the truck's dwell time window, ensuring that they occur strictly after the completion of the truck's battery-swapping operations. Constraints (39) and (40) explicitly isolate and quantify the actual grounded idle waiting time of the UAV and the stationary idle waiting duration of the truck, respectively, which are induced by temporal asynchrony during physical spatio-temporal synchronization.

Fresh Produce Quality Decay Constraints:

$$T_{high}^{i} \geq T_{high}^{j} + \left(A_{j}^{drone} - A_{i}^{drone}\right) - M\left(1 - y_{ij}\right), \forall i, j \in N_{drone} \tag{41}$$

$$T_{high}^{i} \geq \left(A_{j}^{drone} + Wait_{j}^{drone}\right) - A_{i}^{drone} - M\left(1 - y_{ij}\right), \forall i \in N_{drone}, \forall j \in N_{truck} \tag{42}$$

$$T_{low}^{i} \geq T_{low}^{j} - M\left(1 - y_{ij}\right), \forall i, j \in N_{drone} \tag{43}$$

$$T_{low}^{i} \geq A_{n+1}^{truck} - A_{i}^{truck}, \forall i \in N_{truck}^{R} \tag{44}$$

$$T_{low}^{i} \geq A_{n+1}^{truck} - \left(A_{j}^{drone} + Wait_{j}^{drone}\right) - M\left(1 - y_{ij}\right), \forall i \in N_{drone}, \forall j \in N_{truck}^{R} \tag{45}$$

Constraints (41) and (42) jointly define the calculation boundaries for ambient-temperature quality decay. They precisely accumulate the inter-node time differentials during multi-visit routing, strictly anchoring the termination epoch of the ambient exposure to the exact instant the cargo arrives at the truck for physical synchronization. Constraints (43) – (45) formulate the spatio-temporal propagation logic of the low-temperature cold chain. By meticulously deducting the preceding ambient exposure time, they ensure that—regardless of whether the fresh produce is directly collected by the truck or transferred via UAV relay—the low-temperature preservation duration for all co-loaded cargo converges uniformly upon the final arrival at the cold storage depot as the absolute temporal baseline.

4 Numerical Experiments

To validate the proposed spatio-temporal decoupling architecture, we construct test instances based on complex mountainous road networks. The models are implemented in MATLAB and solved using IBM ILOG CPLEX 12.10. All experiments were conducted on a workstation with an AMD Ryzen 7 5800H (3.20 GHz) processor and 16 GB RAM, setting a 3600-second time limit and a 0.05 MIP relative gap tolerance.

4.1 Experiments

We conducted a comparative analysis between the decentralized battery-swapping mechanism proposed in this paper and the traditional truck-only battery-swapping mechanism in which the UAV can only swap batteries on the truck. The core operational metrics are compared in Table 2. As evidenced by the logs in Table 2 and the macroscopic topological evolution in Figure 1, decentralized battery-swapping stations serve not only as physical lifelines for short-endurance UAVs but also as core catalysts to reduce the rigid spatio-temporal coupling between the truck and the drone.

Table 2. Comparison of Core Metrics: Decentralized vs. Truck-only Battery-Swapping.

	Total Cost	Truck Wait Cost	Low-Temp Decay Cost
Truck-only battery-swapping	464.72	23.84	113.27
Decentralized battery-swapping	415.58	11.80	62.83

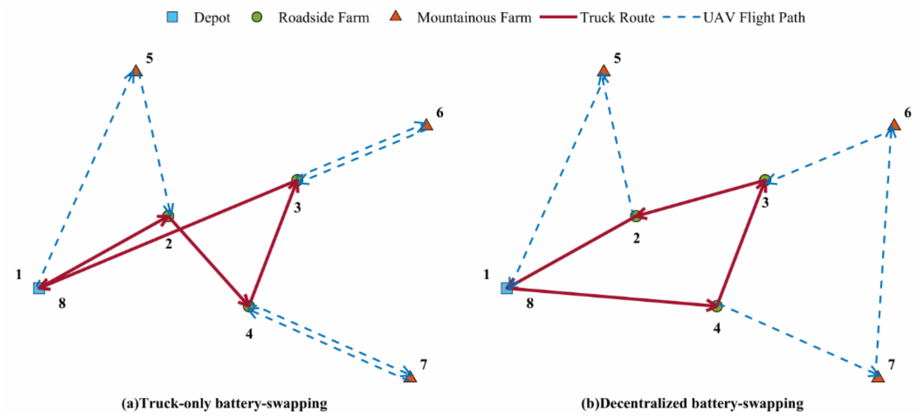

Fig. 1. Topological Evolution of Routing Paths: Truck-only vs. Decentralized.

As illustrated in Figure 1(a), under the truck-only battery swapping strategy, the UAV loses its capacity for independent energy replenishment in remote areas, and its flight trajectories are rigidly confined within the physical radius of the truck. Faced with remote mountainous farm clusters (Nodes 6 and 7), the UAV is compelled by an inescapable "return gravity" toward the primary roadside artery after completing heavy-load collections, due to the lack of intermediary energy replenishment. This results in inefficient "origin-based rapid turnarounds" (e.g., paths 4→7→4 and 3→6→3). This underlying energy bottleneck causes a severe dimensionality reduction in the proposed spatio-temporal decoupling architecture, relegating the truck to a mere cumbersome energy-replenishment vehicle and landing pad. System logs indicate that the truck accumulates up to 47.68 minutes of ineffective idle waiting at various nodes while awaiting the UAV's return for synchronization.

By contrast, under the decentralized battery swapping strategy (Figure 1(b)), the system transcends the energy constraints of the truck, autonomously optimizing and executing a battery-swapping operation at the heavily loaded remote Node 6. Logs show that the UAV arrives at Node 6 in a critical low-power state (remaining energy: 87.31 Wh), but instantaneously recovers to full capacity (3968.80 Wh) by swapping batteries at Node 6. This minor infrastructural intervention directly triggers a benign phase transition in the macroscopic topology: the UAV completely breaks free from the physical anchors of the truck, executing highly autonomous and wide-area multi-visit routing (i.e., the closed-loop link of 4→7→6→3).

Under this extreme release of spatial flexibility, the truck is fully liberated. It no longer requires rigid "dead-waiting" strategies at each node, but instead seamlessly executes a highly efficient counter-clockwise peripheral sweep of 1→4→3→2→8. This reduces the network-wide truck idle waiting costs by a staggering 50.50% (to 11.80 CNY). Furthermore, the improved circulation efficiency of the truck significantly shortens the in-transit time for fresh produce, leading to a 44.53% decrease in quality decay costs during the low-temperature preservation phase (dropping from 113.27 CNY to 62.83 CNY). Ultimately, the total system operational cost is reduced by 10.57%.

The experimental results show that strategically pre-positioning independent battery-swapping resources in complex mountainous scenarios can leverage immense spatio-temporal scheduling dividends for the entire truck-drone collaborative network at a minimal marginal infrastructure cost. This serves as a critical managerial lever for eliminating the "bottleneck effect" in collaborative routing and enhancing the resilience of fresh produce logistics.

4.2 Computational Performance and Scalability Analysis

To evaluate the scalability and computational efficiency of the proposed MILP model, this study tests the algorithm across varying network dimensions ranging from 8 to 20 nodes. Consistent with the aforementioned experimental setup, the IBM ILOG CPLEX solver is constrained by a 3600-second time limit and a 0.05 MIP relative gap tolerance. The computational performance, evaluated by the CPU solving time and the final optimality gap, is illustrated in Figure 2.

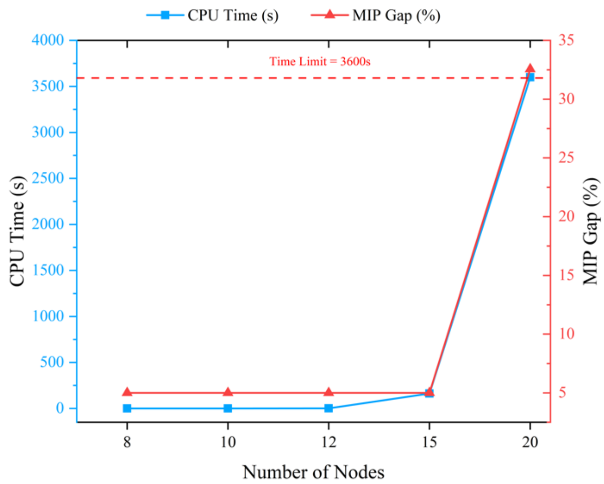

Fig. 2. CPU Time and MIP Gap variations with increasing network nodes.

As visualized in Figure 2, the trajectory of the operational performance exhibits a distinct phase transition. For small to medium-sized networks (8 to 15 nodes), the proposed model demonstrates exceptional tractability. The solver efficiently closes the upper and lower bounds, terminating once the relative MIP gap falls strictly below the pre-set 0.05 tolerance limit. Notably, instances with up to 12 nodes are solved almost instantaneously (within 2 seconds), and the 15-node instance achieves an optimal solution within 162.55 seconds. Consequently, these instances form a perfectly horizontal line at the 5% mark on the secondary Y-axis.

However, when the network scales to 20 nodes, the computational time (primary Y-axis) undergoes a severe exponential explosion, hitting the 3600-second computational wall. Correspondingly, the solver fails to reach the predefined tolerance within the time limit, resulting in a residual gap of 32.55%. This abrupt dimensionality explosion empirically validates the NP-hard nature of the single-truck-single-drone routing problem. The integration of continuous payload-aware energy tracking, Arrhenius quality decay dynamics, and strict spatio-temporal synchronization for decentralized battery-swapping significantly intensifies the combinatorial complexity. While the exact solver provides a rigorous global optimal boundary for smaller instances, these results strongly underscore the necessity of developing highly efficient adaptive heuristic algorithms to handle large-scale collaborative pickup and delivery operations in future applications.

5 Conclusions and future research

Centered on the "decentralized battery-swapping mechanism" and integrating payload-aware energy consumption alongside Arrhenius quality decay dynamics, this paper proposes a high-fidelity collaborative single-truck-single-drone routing optimization model for fresh produce collection. Experiments show that the proposed architecture completely liberates 3D spatial flexibility by successfully decoupling the UAV's physical dependence on the truck through the pre-positioning of independent battery-swapping resources at remote farms. This infrastructure decentralization, achieved at a minimal marginal cost, drastically reduces the truck's ineffective idle waiting time by 50.50%, significantly enhancing global circulation efficiency and driving a 44.53% reduction in low-temperature quality decay costs. This presents a critical managerial implication: in complex terrains, moderately investing in lightweight decentralized energy infrastructure serves as the ideal lever to unlock massive operational scheduling dividends and eliminate the "bottleneck effect" in collaborative routing.

Constrained by the computational capability bottlenecks of exact commercial solvers when handling complex spatio-temporal decoupling constraints, the current scope of this study primarily focuses on the single-truck and single-drone mode to obtain rigorous global optimal boundaries. Future research can be further extended to construct multi-truck and multi-drone collaborative pickup and delivery models, accompanied by the development of highly efficient adaptive heuristic algorithms suitable for large-scale problem instances. This will enable deeper exploration into the swarm collaborative trade-offs of multi-truck multi-drone fleets within mountainous fresh produce logistics networks, as well as the joint optimization of decentralized battery-swapping station location and routing.

References

1. Murray, C., Chu, A.: The flying sidekick traveling salesman problem: Optimization of drone-assisted parcel delivery. Transportation Research Part C: Emerging Technologies 54, 86-109 (2015)
2. Wang, Z., Sheu, J.: Vehicle routing problem with drones. Transportation Research Part B: Methodological 122, 350-364 (2019)
3. Shi, Z., Hong, S., Wang, Z., Li, A.: Exact solution approaches for the traveling salesman problem with a drone station. European Journal of Operational Research 328, 845-861 (2025)
4. Jiang, Y., Liu, M., Jia, X., Xue, Q.: The multi-visit vehicle routing problem with multiple heterogeneous drones. Transportation Research Part C: Emerging Technologies 172, 105026 (2025)
5. Mulumba, T., Diabat, A.: Optimization of the drone-assisted pickup and delivery problem. Transportation Research Part E: Logistics and Transportation Review 181, 103377 (2024)
6. Alizadeh, A., Srinivas, S., Noble, J., Otto, A.: Collaborative truck multi-drone pollution routing problem with pickup and delivery under variable truck speeds: A cost minimisation approach. International Journal of Production Research 1-33 (2026)
7. Meng, S., Chen, Y., Li, D.: Pickup and delivery problem with multi-visit drones considering soft time windows. Transportation Research Part C: Emerging Technologies 180, 105359 (2025)

8. Lyu, M., Liu, W., He, Q., Wu, L.: Urban food delivery service optimisation with coordinated delivery riders and drones. Transportation Research Part E: Logistics and Transportation Review 204, 104412 (2025)
9. Zhang, J., Li, Y.: Collaborative vehicle-drone distribution network optimization for perishable products in the epidemic situation. Computers & Operations Research 149, 106039 (2023)
10. Stellingwerf, H., Groeneveld, L., Laporte, G., Kanellopoulos, A., Bloemhof, J., Behdani, B.: The quality-driven vehicle routing problem: Model and application to a case of cooperative logistics. International Journal of Production Economics 231, 107849 (2021)
11. Yin, Y., Li, D., Wang, D., Ignatius, J., Cheng, T., Wang, S.: A branch-and-price-and-cut algorithm for the truck-based drone delivery routing problem with time windows. European Journal of Operational Research 309(3), 1125-1144 (2023)
12. Gu, R., Liu, Y., Poon, M.: Dynamic truck-drone routing problem for scheduled deliveries and on-demand pickups with time-related constraints. Transportation Research Part C: Emerging Technologies 151, 104139 (2023)
13. D'Andrea, R.: Guest Editorial Can Drones Deliver? IEEE Transactions on Automation Science and Engineering, 647–648 (2014)
14. Meng, S., Guo, X., Li, D., Liu, G.: The multi-visit drone routing problem for pickup and delivery services. Transportation Research Part E: Logistics and Transportation Review 169, 102990 (2023)
15. Yurek, E., Ozmutlu, H.: Traveling salesman problem with drone under recharging policy. Computer Communications 179, 35-49 (2021)
16. Kitjacharoenchai, P., Min, B., Lee, S.: Two echelon vehicle routing problem with drones in last mile delivery. International Journal of Production Economics 225, 107598 (2020)